Innovative architectures in ferroelectric multi-materials: Chemistry, interfaces and strain

C. Elissalde[*,§], U.-C. Chung[*], G. Philippot[*], J. Lesseur[*], R. Berthelot[*], D. Sallagoity[*,‡], M. Albino[*], R. Epherre[†], G. Chevallier[†], S. Buffière[*], A. Weibel[†], D. Bernard[*], J. Majimel[*], C. Aymonier[*], S. Mornet[*], C. Estournès[†] and M. Maglione[*]

[*]*CNRS, Univ. Bordeaux, ICMCB, UPR 9048, F-33600 Pessac, France*

[†]*CNRS, Univ. Toulouse, UPS, INP, Institut Carnot Cirimat, F-31602 Toulouse, France*

[‡]*ICMN, Univ. Catholique deLouvain, B-1348, Louvain-la-Neuve, Belgium*

[§]elissald@icmcb-bordeaux.cnrs.fr

Breakthroughs can be expected in multi-component ceramics by adjusting the phase assembly and the micro–nanostructure. Controlling the architecture of multi-materials at different scales is still challenging and provides a great opportunity to broaden the range of functionalities in the field of ferroelectric-based ceramics. We used the potentialities of Spark Plasma Sintering (SPS) to control a number of key parameters regarding the properties: anisotropy, interfaces, grain size and strain effects. The flexibility of the wet and supercritical chemistry routes associated with the versatility of SPS allowed designing new ferroelectric composite ceramics at different scales. These approaches are illustrated through various examples based on our work on ferroelectric/dielectric composites.

Keywords: Ceramics; composites; nanostructures; ferroelectric; dielectric; spark plasma sintering; structure-property relationships.

1. Introduction

Ferroelectric oxides are functional materials widely used as passive components in microelectronic devices. In mobile electronics, antagonistic issues must be resolved as new functionalities are requested (internet, camera, MP3) while the available space for their development is decreasing. If transistors and magnetic materials reach today a high degree of integration, it is not the case for the passive components (capacitors, resonators, filters, piezoelectric transducers, etc.). The current trend aims developing new nanosized components or devices able to achieve several functions such as tunable materials, which are presenting variable characteristics according to the applied electric field. Among them, ferroelectric oxides are promising candidates due to their high permittivity and nonlinear properties. High permittivity allows the size reduction of components, which is an obvious advantage for radio frequency and microwave applications. However, to extend the range of applications it is desirable to lower the permittivity while keeping the tunability (defined as the variation of permittivity under an applied electric field). The properties of ferroelectric based-ceramics are intrinsically related to their crystal structure, chemical composition, and nano/microstructure as well as to the distribution and the scale of heterogeneities (impurities, defects, dopants, etc.) they contain. Modifying both the composition and the microstructure allows properties adjusting.[1] The Curie temperature can be tuned continuously around room temperature thanks to suitable ionic substitutions. Grain size is an additional key parameter to fix both the transition temperatures and the permittivity values.[2,3] To fit with the huge expectations in terms of frequency broadening, another challenge is also to control the dielectric losses in a wide frequency range. As a result, materials are designed with more and more complex structures over several spatial scales, and their final effective performances are strongly correlated to the control level of their structuration during synthesis and shaping.

During the last 20 years significant progress in processing dense nanostructured ceramics was achieved.[4–7] Ferroelectric nanopowders with a grain size below 20 nm are now available but the processing routes used are mainly focused on barium titanate (BT).[8–10] Producing well-crystallized sub-50 nm grains of narrow size distribution and over a whole solid solution is still a challenge. In addition, several works in literature, underline the spreading of the permittivity values and highlight the strong influence of both synthesis and sintering methods.[11] The requirement of achieving high-density ceramics while keeping nanoscale grain size has led to an increasing interest on advanced sintering techniques. In particular, Spark Plasma Sintering (SPS) is nowadays well recognized as a very efficient tool to yield functional ceramics

with controlled micro–nanostructures.[12] Highly densified ferroelectric ceramics with grain size lower than 100 nm are now currently obtained using fast sintering techniques.[12–16] However, producing ceramics made of sub-50 nm grains while minimizing extrinsic contributions to the dielectric properties remains a difficult task. Both the quality of the initial nanopowders (crystallinity, stoichiometry, hydroxyl groups) and the control of charged defects (oxygen vacancies, free electrons) in the final ceramics are mandatory to improve dielectric performances. The flexibility of SPS in terms of experimental parameters (pressure, electric current, heating and cooling rates) allowed extending the range of functionalities in ferroelectric materials within particular the control of chemical diffusion[17] and charged defects in ceramics.[18] Strain and interfaces can also be exploited in ferroelectric materials to tailor their properties and it is then possible to evaluate the effects of the external stress (external tunable load applied during SPS) on the local structure of nanostructured ferroelectrics ceramics with grain size below 20 nm.[19]

Through various examples, we will first emphasize the great potential of combining wet chemistry synthesis routes with SPS to perform nanoscale-designed ferroelectric ceramics. The wet and supercritical chemistry routes enable the synthesis of well-crystallized ferroelectric nanoparticles and are also suitable to design coated ferroelectric particles. The impact of the nanostructure, grain size and defects chemistry on dielectric losses and permittivity values of the SPS ceramics will be discussed.

In a second part, we will present ferroelectric/dielectric composites designed at the micro-scale. The characteristics of the dielectric phase, the control of the ferroelectric matrix at different scales and the versatility of SPS allow to generate original microstructures. The effective ferroelectric properties are controlled by the spatial distribution of the different phases, their connectivity and microstructural anisotropy. We will emphasize the possibilities offered by 3D imaging techniques at microscale (X-ray computed microtomography (XCMT)) to characterize the architecture of multi-materials in 3D for different crucial steps of their processing and correlate the morphology of the dielectric material with the ferroelectric properties.

2. Experimental Procedure

The ferroelectric particles used in the different studies (BT, $Ba_{1-x}Sr_xTiO_3$ (BST)) with grain size ranging between 50 and 500 nm) were either commercial powders or synthesized by solid-state route and under supercritical conditions using a continuous-flow reactor.[20,21]

2.1. *Multi-materials at the nanoscale*

Different synthesis routes were followed to coat the ferroelectric particles according to the nature and the crystallinity of the dielectric shell.

The seed growth process was used to encapsulate by silica each ferroelectric particle. This soft chemistry route, derived from the so-called Stöber process, ensures a uniform, continuous and homogeneous nanoscale silica coating (from 1 to 100 nm) whatever the size and the shape of the ferroelectric cores.[22] Further functionalization is possible leading to raspberry design generated by electrostatic interactions and consisting of silica coated ferroelectric particles surrounded by an assembly of silica coated magnetic nanoparticles (γ-Fe_2O_3@SiO_2).[23]

The coating of ferroelectric nanoparticles with a shell of few nanometers of amorphous alumina was performed using the supercritical fluid chemical deposition process (SFCD).[24] Indeed, under the operating conditions (i.e., 20 MPa, 170°C, CO_2/ethanol (80/20 molar), residence time 1 h) the mixture CO_2/ethanol is supercritical (Pc mixture = 14.5 MPa, Tc mixture = 92°C).

To obtain crystallized MgO shell around the BT particles, a thermolysis process was developed. The reaction occurs by thermal decomposition of the magnesium precursor during heating at around 290°C under reflux and the crystallized MgO nanosized particles aggregate around BT particles.[25]

The core@shell samples were sintered using the SPS equipment Dr Sinter SPS-2080 (Syntex Inc.) located at CNRS-PNF2 (PlateformeNationale de Frittage Flash, CIRIMAT Toulouse, France). The sintering cycles consisted in heating rates of 100°C/min, a dwell of 3 min at the sintering temperature (1100°C) and an uniaxial load (50 MPa) gradually applied during the last minute of temperature increase. The sintering was carried out under vacuum (down to 6 Pa). The electrical pulse pattern consisted of 12 current pulses (one pulse duration 3.3 ms) followed by two periods (6.6 ms) of zero current. In the case of BT@SiO_2 powders, densification was also achieved by SPS at lower temperature (1050°C) and under neutral atmosphere (argon). A post annealing in air at 800°C was performed to remove surface carbon contamination and reoxidize ceramics.

2.2. *Ferroelectric/dielectric composites at the microscale*

Composites made of MgO dielectric inclusions in a ferroelectric $Ba_{0.6}Sr_{0.4}TiO_3$ (BST) matrix were fabricated to lower the dielectric losses while maintaining permittivity tunability. BST particles were mixed with spheroidal spray-dried granules of MgO with diameters in the range 10–100 μm. Each granule is composed of packed elementary crystallites of nanometer size. The mixed powders were sintered by SPS (device described in Sec. 2.1) under vacuum and applying a uniaxial pressure of either 50 MPa or 100 MPa at the sintering temperature (1200°C). We used the possibilities offered by XCMT to propose a complete quantitative description of the ferroelectric composites. 3D imaging on the real microgeometry (initial powder mixing and final microstructure) was obtained using synchrotron radiation from ESRF (European Synchrotron Radiation Facility, Grenoble,

France, 3D imaging beamline ID19) and from SLS (Swiss Light Source, Villigen, Switzerland, 3D imaging beamline TOMCAT).

3. Results and Discussion

3.1. *Composites designed at the nanoscale*

In this first part are described the strategies used to design nanostructured composites with tailored dielectric properties. The proposed core–shell concept aims to build a network made of ferroelectric particles individually coated with a shell made of a dielectric oxide. A full control of both the size of the ferroelectric core (BT, BST) and the thickness of the non ferroelectric shell (SiO_2, Al_2O_3, MgO) is mandatory to control the final ceramic properties. The modification of particle surfaces described by Caruso as "particle nanoengineering" is a powerful tool that offers a fine control of magnetic, optical, electronic and catalytic properties at the nanoscale.[26] The coating of oxide or metallic particles with a continuous silica shell (core@shell architecture) has led to significant advances in functional materials increasing drastically their range of applications. This concept has already been applied to various inorganic materials from magnetic materials (Fe_2O_3@SiO_2)[27] to structural oxides (Al_2O_3@SiO_2).[28] Focussing on bulk ferroelectric materials, such a core–shell approach has been increasingly explored these last years in order to initiate solid-state reaction at the nanoscale,[29] to monitor densification including the control of grain coarsening, and to tune the macroscopic properties.[30] In our pioneer work, silica was initially selected as coating material because it acts as an efficient dielectric loss barrier at the grain scale.[22,17] The seed growth process used for the silica coating, allows an accurate control of the shell thickness (Fig. 1(a)). The most striking effect arises from the possibility to fully control the functionalities through the sintering

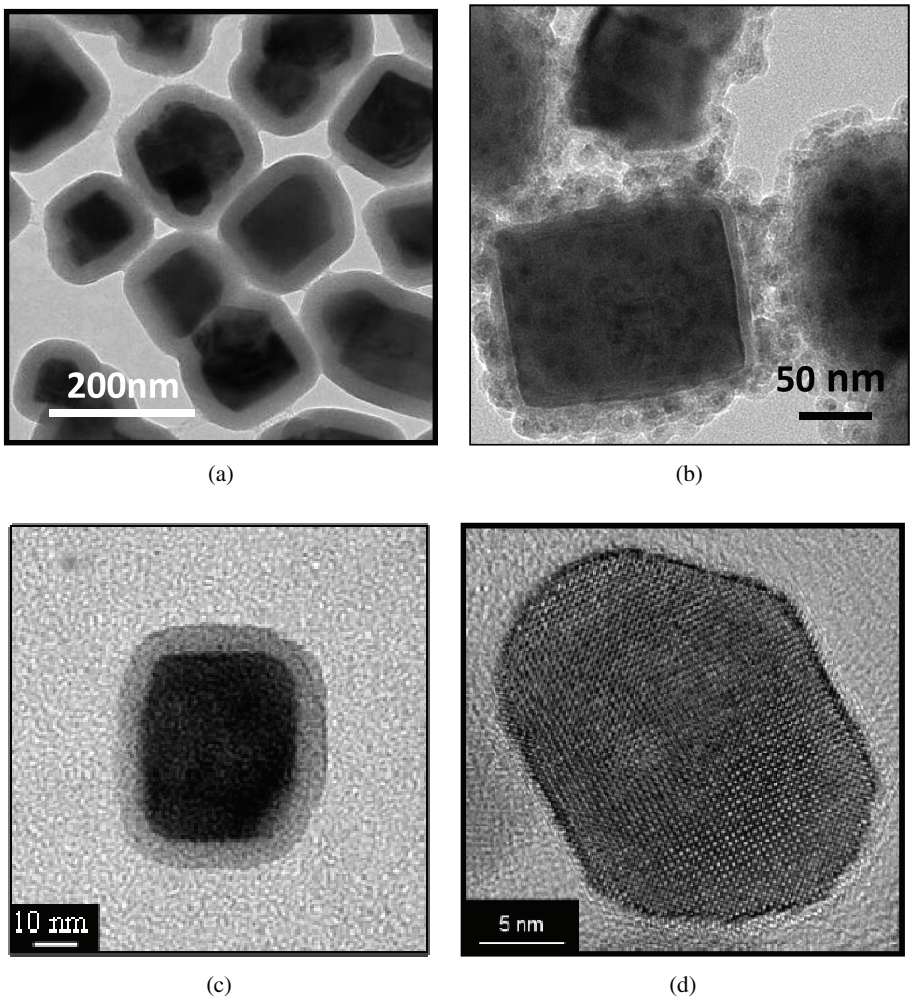

(a) (b)

(c) (d)

Fig. 1. (a) TEM image of BST nanoparticles coated with silica shell using a method based on a seeded growth process. (b) TEM image of raspberry nanoparticles: BT@SiO_2 core surrounded by γ-Fe_2O_3@SiO_2 nanocrystals. (c) TEM image of BST nanoparticle coated with Al_2O_3 using supercritical fluid chemical deposition process. (d) TEM image of BT nanocrystal synthesized using supercritical chemistry route.

conditions. Starting from the same initial core–shell ($BaTiO_3$@SiO_2) particles, we were able to obtain different functionalities simply by adjusting the SPS sintering conditions (atmosphere, sintering temperature) (Fig. 2). Sintering performed under inert atmosphere (argon) and at low temperature (1050°C) enables to obtain low temperature dependence of the permittivity and low dielectric losses. Using HRTEM to probe the interface between the two components, an accurate control of the interphase formation was possible at the atomic scale. The fresnoite, $Ba_2TiSi_2O_8$, was clearly identified as a secondary phase growing in-between the two components.[17,31,32] When the sintering is performed under reducing conditions (vacuum) with a slight increase of the sintering temperature (1100°C), ceramics properties exhibit giant permittivity.[18]

In the actual context of an increased demand of novel energy sources, ceramics with giant permittivity are promising candidates as supercapacitors. $BaTiO_3$ ceramics exhibiting huge effective dielectric parameters were reported in literature,[33,34] when appropriately substituted or when the grain size decreased under fast sintering conditions. In all these cases, the apparent dielectric permittivity is quite high at room temperature ($> 10^5$ in some cases), and is temperature independent in a broad range before falling down at low temperatures. While these features are very appealing for applications, some parameters are still not controlled: the dielectric losses are usually high and the low frequency contributions to the dielectric permittivity are ascribed to dc conductivity. If higher permittivity improves the amount of charges that can be stored, low dielectric losses for the material are required to stand high power density. The main advantage of coating each ferroelectric particle with silica is to accurately control the grain boundaries. Such coating is not only efficient for the decrease of dielectric losses but also to control the reduction state of the inner grains. When the composite is sintered under low oxygen partial pressure, the reduced ferroelectric core (creation of oxygen vacancies and associated Ti^{4+} reduction into Ti^{3+}) is trapped into the silica barrier and the post thermal treatment usually performed to re-oxidize the ceramic is inefficient. The silica shell acts thus as an oxygen diffusion barrier. As a result, permittivity as high as 150,000 are obtained while dielectric losses remain moderate (5%) and stable all along the temperature range. The post-annealing treatment can be optimized in order to keep the gain in permittivity while restoring its maximum at the Curie temperature. A space charge relaxation was observed at low temperature and a close link between the macroscopic dielectric relaxation and the microscopic dynamics of charged defects (Ti^{3+}-VO) was clearly evidenced using Electron Paramagnetic Resonance.[35]

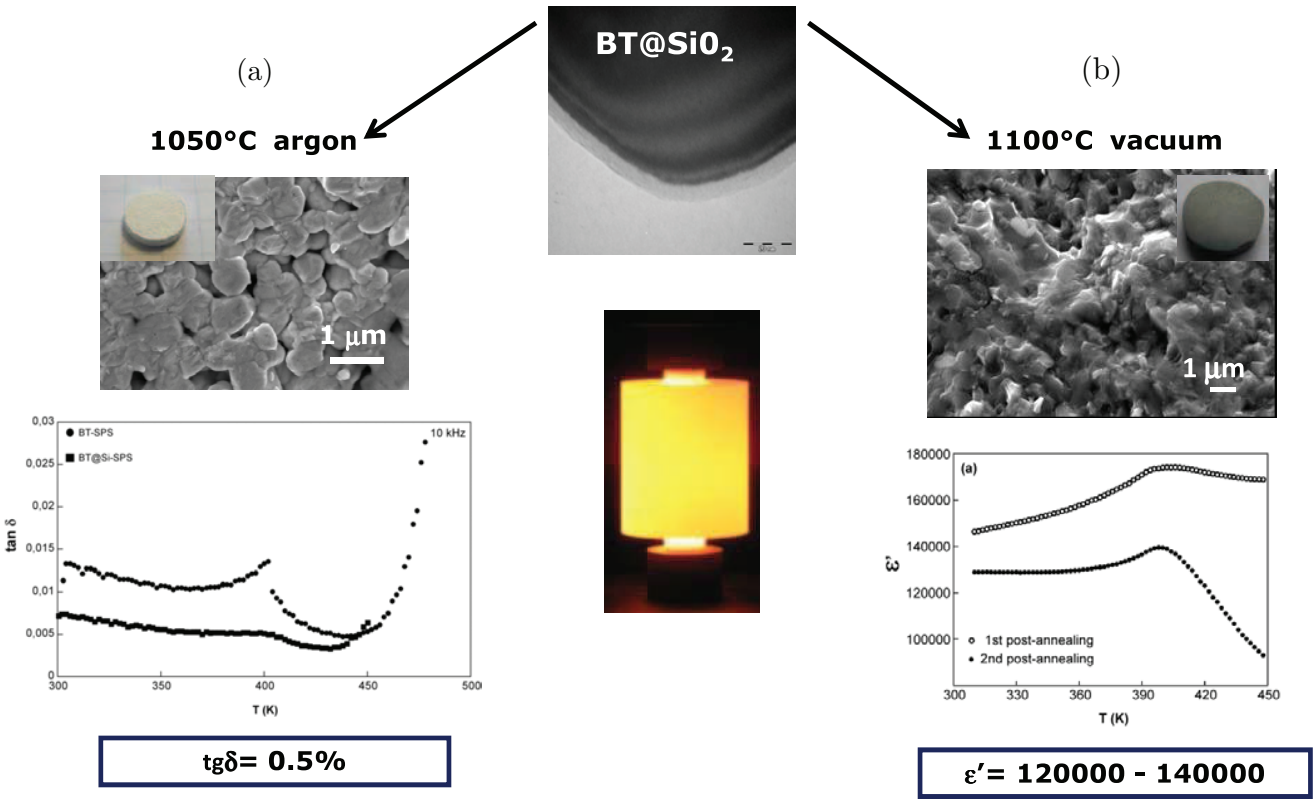

Fig. 2. (a) and (b) SEM images of ceramics made of BT@SiO_2 nanoparticles sintered by SPS in different conditions (temperature and atmosphere) and corresponding dielectric properties ((a) losses temperature dependence of uncoated BT and BT@SiO_2 ceramics, (b) permittivity temperature dependence of BT@SiO_2 ceramics after annealing).

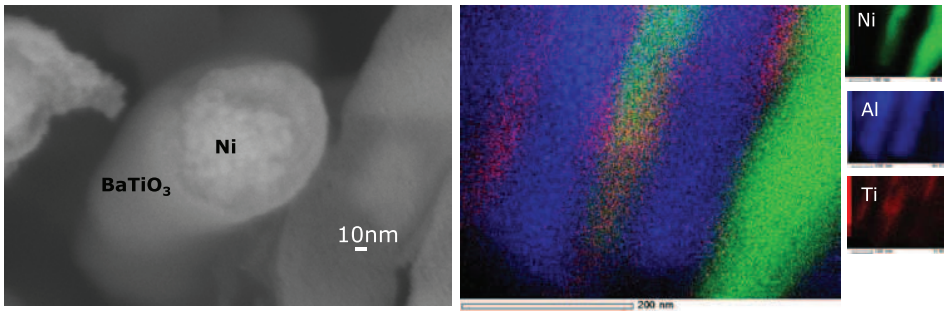

Fig. 3. SEM image of $Ni@BaTiO_3$ nanocable and chemical mapping of nanocable within alumina template.

The silica coating allows a further functionalization of the nanoparticles enabling to target the elaboration of magneto-electric compounds. Complex structures such as nanopilars of $CoFe_2O_4$ embedded in $BaTiO_3$ thin films on a $SrTiO_3$ substrate were already studied.[36] Thanks to the lattice distortion of the $BaTiO_3$ matrix, the magnetic susceptibility of the spinel grains was perturbed at the ferroelectric transition temperature of $BaTiO_3$. This showed that not only the nanocomposites displayed ferromagnetic and ferroelectric hysteresis loops but also a coupling between these two parameters is achieved through elastic interactions. Such a two-dimensional (2D) approach requires a substrate to clamp the film in the substrate plan to generate the distortion in the perpendicular direction, resulting from the ferroelectric transition, which leads to the magneto-electric coupling. Our aim was to process three-dimensional (3D) nanocomposites by intimately mixing, ferroelectric cores with magnetic grains through silica $[BST@SiO_2 - \gamma\text{-}Fe_2O_3@SiO_2]$ to obtain co-existence of ferroelectricity and ferromagnetism in a bulk ceramic (Fig. 1(b)). Nanoraspberry morphologies are formed by electrostatic interactions between the two colloidal mixed systems. Taking advantage of the silica used here as a sticking agent between the two metal oxide phases, the coalescence between ferroelectric particles can be prevented, phase transition behavior of magnetic core can be avoided through size control and neck formation is favored during the densification step by increasing the solid–solid interfaces. As a result, sintering occurs at lower temperature preventing thus the final grain growth. Multi-functionality in terms of coexistence between ferroelectric and superparamagnetic properties was demonstrated.[23]

A main advantage of the core@shell approach lies in the existence of extended interfaces between the components in all directions, this is believed to promote the magneto-dielectric coupling. Alternatively to the architectures mentioned above, the core–shell approach can be also exploited in one-dimensional (1D) nanostructures that coaxially combine electric and magnetic materials. This flexible approach is illustrated through the elaboration of high density $Ni@BaTiO_3$ nanocable arrays. We have combined electrochemical deposition and wet chemical impregnation processes within a highly ordered unidirectional porous alumina (AAO) membranes.[37] Core–shell multiferroic nanocables, that are very difficult to obtain using conventional lithographic techniques, are elaborated with compositions, morphologies and geometrical parameters controlled to a large extent. Magnetoelectric coupling through mechanical coupling can be expected considering such arrays of vertically aligned core–shell nanocables having large interface area. Ni nanowires were grown within the BT nanotubes, obtained by wetting the AAO membrane with barium titanate sol and subsequent annealing (Fig. 3). The versatility of this approach lies in the tunability of the nanocable length, the core diameter, the ferroelectric tube wall thickness, and thus the packing density of the Ni nanowires. The core–shell structure was investigated by Bright field Scanning Transmission Electron Microscopy coupled with Energy Dispersive X-Ray Spectroscopy (Fig. 3). The strength of the magnetic dipolar interaction arising from the packing density of the magnetic nanowires was correlated to the $BaTiO_3$ wall thickness through magnetometry and ferromagnetic resonance measurements.[37]

SFCD process was also used to functionalize $BaTiO_3$ nanoparticles with an amorphous Al_2O_3 shell of few nanometers (Fig. 1(c)).[24] Versatility in both alumina structure and crystallinity, and particle architecture is obtained simply by changing the reaction parameters.[38] The sintering of the as-obtained powders was studied as a function of the inter-diffusion between the ferroelectric core and the alumina phase. Fast sintering of the core–shell nanoparticles was used to control interphase occurring at the interface between the ferroelectric and dielectric materials and the final ceramic exhibited significant improvement in the lowering of dielectric losses while keeping the BT Curie temperature unchanged.

Using an ethanol/water supercritical mixture as reaction media, it is also possible to synthetize multi-cation oxides with an accurate control of the composition, the morphology and the structure. Ferroelectric cores with a large range of compositions over a whole solid solution can be thus be synthesized through the supercritical route. The high nucleation and low crystal growth rates achieved lead to ultrafine particles. Compared to various wet chemical methods such as sol–gel processes, co-precipitation and hydrothermal

methods, well-crystallized particles can be obtained directly without tedious washing, filtering or calcination steps. Moreover, the low surface tension of the supercritical fluid allows minimizing aggregation problems encountered in conventional wet chemistry processes. This synthesis route was used to prepare all the compositions belonging to the BST and $BaTi_{1-x}Zr_xO_3$ (BTZ) systems.[20,21,39–42] Nanoparticles with a high purity, crystallinity and grain size below 20 nm as well as narrow particle size distribution can be synthesized under supercritical conditions using a continuous-flow tubular reactor (Fig. 1(d)). The experimental conditions including solvent nature, temperature and pressure can be easily modified to improve particle crystallization, without $BaCO_3$ contamination. SPS was shown to be the most appropriate sintering technique to obtain dense ceramics while preserving the initial nanocrystal size.

Through these different investigations focused on nanostructured ferroelectric materials, we have confirmed the potentiality of the ferroelectric oxide functionalization to tailor properties. However, the main drawback of amorphous coating is the limited sintering temperature and the occurrence in the early sintering stage of interphase between the core and the shell. This has motivated the design of crystallized MgO coating.

The coating method used to obtain a complete MgO crystallized shell onto the ferroelectric nanosized particles was the thermolysis process. STEM-EDX provides a nanoscale chemical probing which confirms the 3D coating, while HRTEM reveals that the shell consists of crystallized nanosized MgO particles randomly oriented. The initial core–shell architecture is transformed into uniform distribution of sub-micrometric sized BT and MgO, *in situ* during SPS (Fig. 4(a)). The weak cohesion of MgO nanocrystallites and their soft plastic behavior under SPS conditions can explain such rearrangement. However, the MgO still acts as a diffusion barrier that prevents the ferroelectric core from grain growth. As a result, dielectric properties reflect the composite effect, with especially low ($\approx 0.5\%$) and stable dielectric losses for a wide frequency range, highlighted by the comparison with BT reference sintered in the same conditions (Fig. 4(b)). The structure of the BT nanoparticles (300 nm) and the Curie–Weiss parameters are also impacted in the composite due to the stress generated during SPS through the extended interfaces between the two components.[25]

3.2. *Multimaterials at the microscale*

To improve the overall behavior of ferroelectrics, two complementary routes have been investigated till now: the chemical one with the use of substitution (BST) or dopants (Mn), and the multi-materials route based on the mixture of a ferroelectric powder and a low loss dielectric oxide such as MgO, $MgTiO_3$, etc.[43–48] Most of these ceramics were

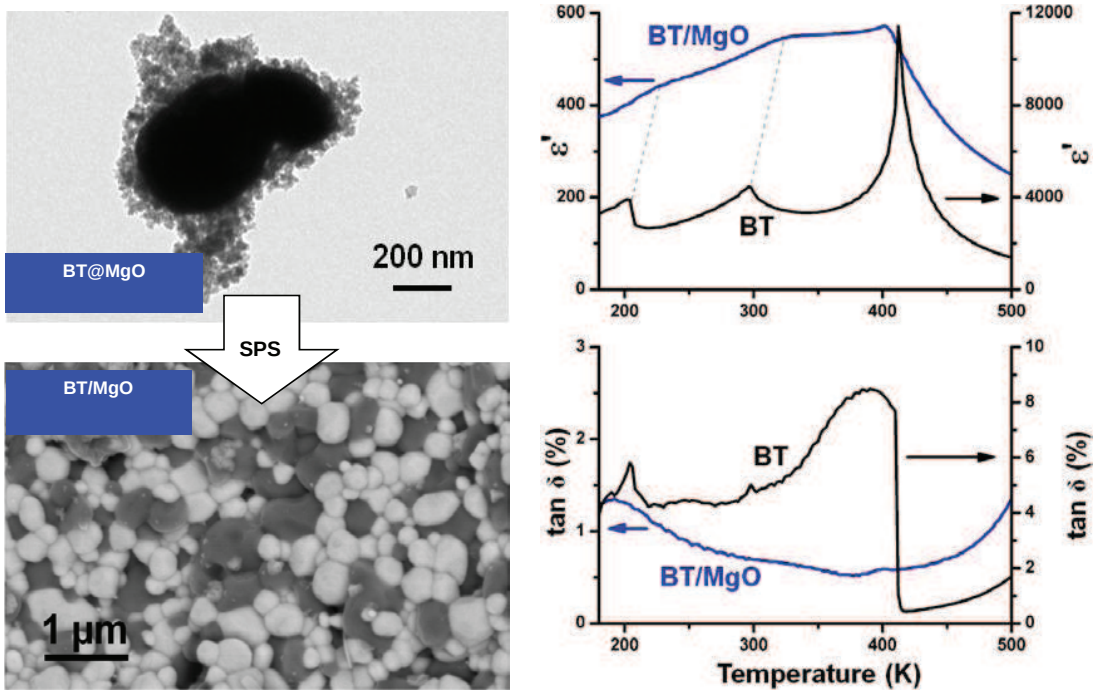

(a) (b)

Fig. 4. (a) TEM image of BT@MgO nanoparticles processed by thermolysis and corresponding sintered nanostructured ceramic by SPS (SEM image in back scattering electron mode: MgO and BT appear in black and white, respectively). (b) Permittivity and losses temperature dependences at 10 kHz: comparison between SPS ceramics made of initially uncoated BT and MgO coated BT.

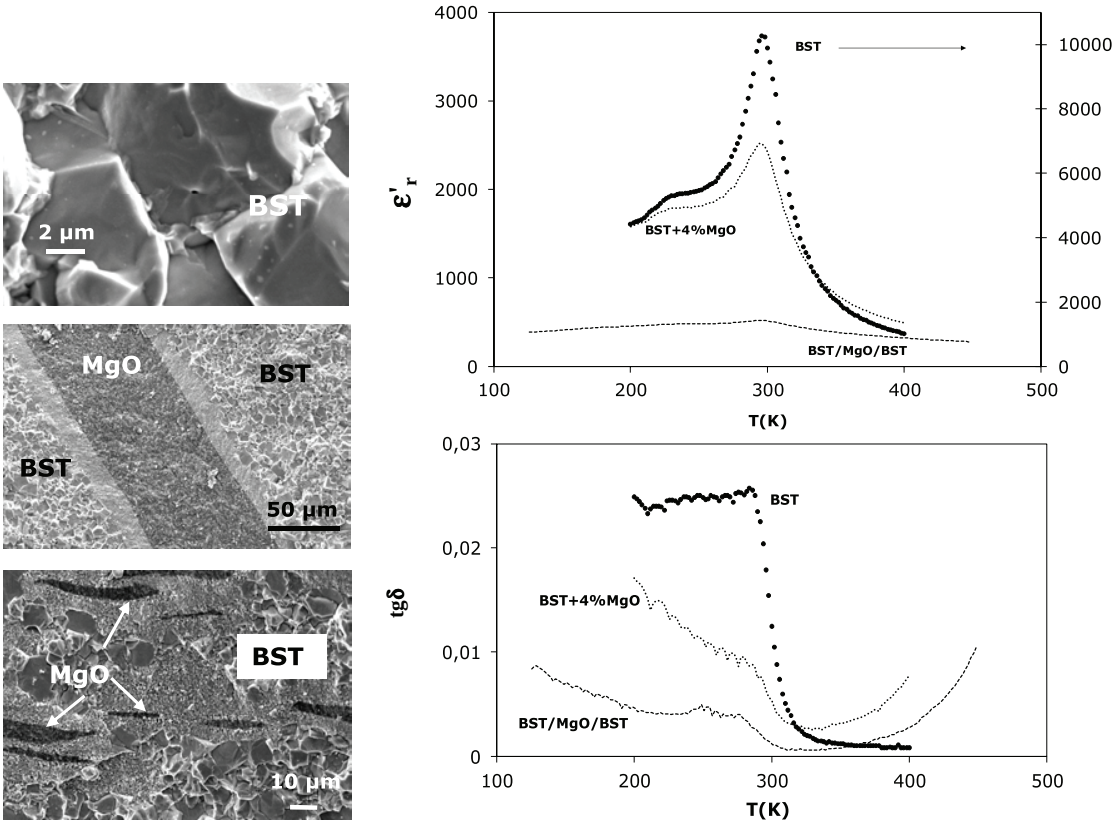

(a) (b)

Fig. 5. (a) SEM images of the fractures of BST, BST/MgO/BST multilayer and 3D BST+4%MgO ceramics sintered by SPS in the same conditions and (b) corresponding permittivity and losses temperature dependences at 10 kHz.

obtained using a conventional sintering process, which implies high sintering temperature and long sintering time to achieve dense composites. As an unavoidable result, inter-diffusion between the two phases led to a decrease of the Curie temperature associated with altered dielectric properties. In addition, using standard sintering there is only a restricted control of the materials chemistry: oxygen deficiency, intrinsic charged defects, valence state. We overcomed these drawbacks using SPS to process highly densified BST/MgO ceramics with different design (multilayer[49] and 3D random mixing[50]). Whatever the connectivity between the two phases and thus increasing the number of interfaces, chemically sharp interfaces are obtained (Fig. 5(a)). Losses were significantly reduced compared to pure BST in the ceramic with a sandwich architecture and a high tunability (40%) at room temperature was obtained in 3D random powders design (Fig. 5(b)).[49,50]

A dual synthesis route was proposed to control simultaneously the extrinsic and intrinsic dielectric losses of barium strontium titanate. The goal is to broaden the frequency range application of these materials by an efficient use of their tunability. Spark plasma sintered ceramics were obtained combining composite and substitution routes. A small addition of magnesium oxide (4 wt.%) as a dielectric phase acts efficiently as a dielectric barrier for grain boundaries extrinsic (low frequency) losses while a 1 mol.% Mn substitution in the ferroelectric matrix effectively lowers the intrinsic (high frequency) losses thanks to electron-trapping by the acceptor Mn defects.[51] The dual scheme combines these effects in a low dielectric losses ($< 1.5\%$) material over a wide frequency range 10 kHz–1 GHz, keeping high tunability (Fig. 6).

Focusing on the 3D BST–MgO composites, we also found an overall dielectric anisotropy, which is new in 3D polycrystalline composites. Very specific microstructure was obtained in these composites due to both the use of initial MgO soft granules and the specific conditions of SPS. The dielectric inclusions can be deformed during high temperature uniaxial compression (1200°C). The mechanical behavior of the MgO granule during sintering process is hardly known. Obviously, SPS kinetics is too fast to be investigated by nondestructive 3D technics such as XCMT. Nevertheless experiments can be performed on the initial powders mixing and on the final ceramic in order to obtain a complete description of the inclusion deformation. In the final SPS ceramic, inclusions with a specific flattened shape (inclusion with a large aspect ratio — flat disk shape) are obtained (Fig. 7). The properties are strongly impacted by the geometry of the dielectric component in the ferroelectric matrix that disturbs the electric field redistribution between the two

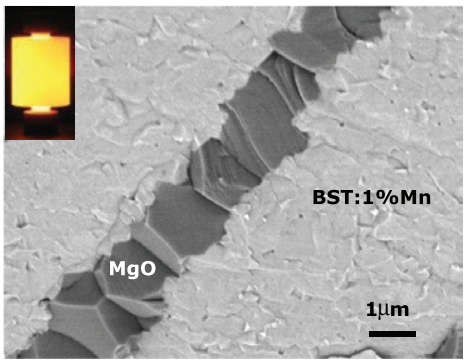

	BST +4%MgO	BST:1%Mn +4%MgO
MgO final grain size	300nm	2 µm
tan (300K – 10kHz)	0.5%	0.6%
tan (300K – 1GHz)	4%	1.4%
Tunability (%) (1kV/mm)	25%	13%

Fig. 6. SEM image of the fracture of BST:1%Mn+4%MgO sintered by SPS and influence of Mn doping on the dielectric characteristics of the composites. BST refers to the composition $Ba_{0.6}Sr_{0.4}TiO_3$.

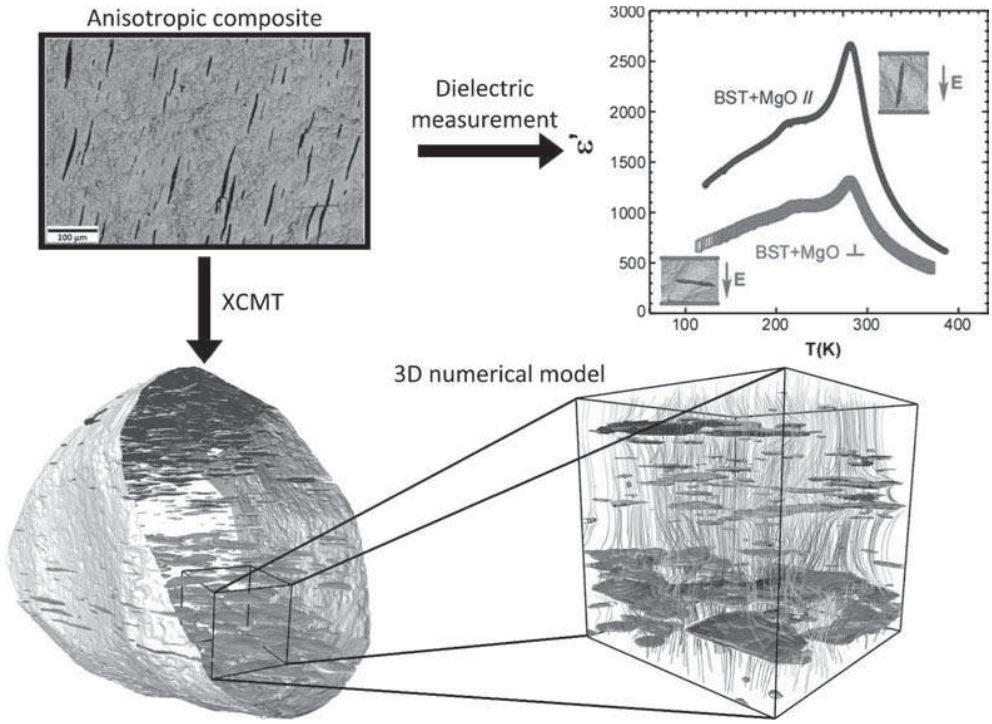

Fig. 7. SEM image of the fracture of BST+4% MgO ceramic sintered by SPS (elongated MgO inclusions appear in black), 3D rendering of the composite (the black cube corresponds to the subvolume used for permittivity computation) and permittivity temperature dependences of the SPS ceramic with electrodes parallel and perpendicular to the inclusion long axis.

components. Using in-depth 3D mapping of the composites through X-ray tomography we pointed out the limits of 2D approach and the capability of handling real 3D microstructures. We have demonstrated that inclusion anisotropy induces anisotropy in the dielectric (Fig. 7) as well as in the piezoelectric and pyroelectric properties of the matrix. Using 3D maps as an input, we could compute the local electric field at the micrometer scale which resulted in an electric field focusing at the dielectric inclusions edges. The 3D simulation was focused on the permittivity at low electric field and compared with Effective Medium Approximations. This is both a confirmation of pre-existing phenomenological models and a first step towards a realistic modeling of such dielectric composites which usually require strong simplifying assumptions.[52]

4. Conclusion

In the field of ceramics for electronics, telecommunications and energy storage, the use of nonlinear high permittivity ferroelectric materials is required for the development of devices such as tunable capacitors and resonators or supercapacitors. Dielectric losses and permittivity are the foremost

parameters for new materials fitting with the rapid evolution of the components in terms of size reduction and frequency range broadening. The composite route is particularly suitable to tailor the final properties provided that both synthesis and sintering steps are well controlled. Linking the architecture, the nano–microstructure and the physical properties allow to increase our fundamental understanding and supports the emergence of innovative functional materials. In this context, our investigations presented here focused on the design, the shaping and the characterization of multi-materials made of ferroelectric ($BaTiO_3$ and derived) and low dielectric losses (SiO_2, MgO, Al_2O_3) phases assembled at the nano and micro-scales. The processing of hierarchical architectures combining materials of different properties at different scales aims at producing adjustable high performance materials. To reach this goal, we have demonstrated the major advantages of advanced processing methods combining the flexibility of the wet and supercritical chemistry routes to process functionalized nanoparticles, and the potentialities of SPS in terms of grain size, constituents assemblies, interfaces and chemical composition control. According to the scale of the ferroelectric/dielectric assemblies processed by SPS, our main objectives were:

— To design core@shell-based multi-materials with a high level of interface control; at the nanometric scale to preserve the initial structure in the final dense ceramic, and at the atomic scale to control charged defects. The shell is considered here as an easily controllable "artificial grain boundaries". This approach enabled not only to tailor different functionalities such as extrinsic and intrinsic dielectric losses and permittivity (up to giant permittivity) but also to open routes towards multi-functionalities with nanorasperry and nanocable architectures.
— To design 3D multi-materials made of dielectric inclusions within a ferroelectric matrix targeting low dielectric losses and high tunability of the dielectric permittivity. Final properties are controlled by the architecture at the micrometric scale leading to an anisotropy of the dielectric inclusions, and also of the intrinsic properties of the ferroelectric matrix. We have highlighted the possibilities offered by 3D imaging techniques at the microscales (XCMT). BST/MgO composites sintered by SPS have anisotropic ferroelectric properties due to the geometry of the dielectric inclusions as demonstrated by 3D numerical modeling of the electric field at the mesoscale.

Acknowledgments

Financial support from the French National Center for Scientific Research (CNRS), the Conseil Régional d'Aquitaine, and the National Research Agency (ANR) (Projects NANO4F (ANR-05-JCJC-0169) and ARCHIFUN (ANR-12-BS08–009) are gratefully acknowledged. We thank M. Paté and J. P. Ganne from Thales Research & Technology, rd. 128, 91767 Palaiseau Cedex, France for tunability measurements.

References

[1] J. Ravez, M. Pouchard and P. Hagenmuller, Chemical bonding and ferroelectric perovskite, *Eur. J. Solid State Inorg. Chem.* **28**, 1107 (1991).
[2] T. Hoshina, Size effect of barium titanate: Fine particles and ceramics, *J. Ceram. Soc. Japan* **121**, 156 (2013).
[3] V. Buscaglia, M. T. Buscaglia, M. Viviani, L. Mitoseriu, P. Nanni, V. Trefiletti, P. Piaggio, I. Gregora, T. Ostapchuk, J. Pokorný and J. Petzelt, Grain size and grain boundary-related effects on the properties of nanocrystalline barium titanate ceramic, *J. Eur. Ceram. Soc.* **26**, 2889 (2006).
[4] H. Zheng, K. Zhu, Q. Wu, J. Liu and J. Qiu, Preparation and characterization of monodispersed $BaTiO_3$ nanocrystals by sol–hydrothemal method, *J. Cryst. Growth* **363**, 300 (2013).
[5] M. T. Buscaglia, M. Bassoli, V. Buscaglia and R. Alessio, Solid-state synthesis of ultrafine $BaTiO_3$ powders from nanocrystalline $BaCO_3$ and TiO_2, *J. Am. Ceram. Soc.* **88**, 2374 (2005).
[6] H.-W. Lee, S. Moon, C.-H. Choi and D. K. Kim, Synthesis and size control of tetragonal barium titanate nanopowders by facile solvothermal method, *J. Am. Ceram. Soc.* **95**, 2429 (2012).
[7] Y. Sakabe, N. Wada and Y. Hamaji, Grain size effects on dielectric properties and crystal structure of fine-grained $BaTiO_3$ ceramics, *J. Korean Phys. Soc.* **32**, S260 (1998).
[8] Y. Li, Z. Liao, F. Fang, X. Wang, L. Li and J. Zhu, Significant increase of Curie temperature in nano-scale $BaTiO_3$, *Appl. Phys. Lett.* **105**, 182901 (2014).
[9] H. Zhang, X. Wang, Z. Tian, C. Zhong, Y. Zhang, C. Sun and L. Li, Fabrication of monodispersed 5-nm $BaTiO_3$ nanocrystals with narrow size distribution via one-step solvothermal route, *J. Am. Ceram. Soc.* **94**, 3220 (2011).
[10] H.-W. Lee, S. Moon, C. H. Choi and D. K. Kim, Synthesis and size control of tetragonal barium titanate nanoparticles by facile solvothermal method, *J. Am. Ceram. Soc.* **95**, 2429 (2012).
[11] S. Yoon, J. Dornseiffer, Y. Xiong, D. Grüner, Z. Shen, S. Iwaya, C. Pithan and R. Waser, Spark plasma sintering of nanocrystalline $BaTiO_3$-powders: Consolidation behavior and dielectric characteristics, *J. Eur. Ceram. Soc.* **31**, 1723 (2011).
[12] F. Maglia, I. G. Tredici and U. Anselmi-Tamburini, Densification and properties of bulk nanocrystalline functional ceramics with grain size below 50 nm, *J. Eur. Ceram. Soc.* **33**, 1045 (2013).
[13] Z. Zhao, V. Buscaglia, M. Viviani, M. Buscaglia, L. Mitoseriu, A. Testino *et al.*, Grain-size effects on the ferroelectric behavior of dense nanocrystalline $BaTiO_3$ ceramics, *Phys. Rev. B.* **70**, 024107 (2004).
[14] M. T. Buscaglia, M. Viviani, V. Buscaglia, L. Mitoseriu, A. Testino, P. Nanni, Z. Zhao, M. Nygren, C. Harnagea, D. Piazza and C. Galassi, High dielectric constant and frozen macroscopic polarization in dense nanocrystalline $BaTiO_3$ ceramics, *Phys. Rev. B.* **73**, 064114 (2006).
[15] T. Hungria, M. Alguero, A. B. Hungria and A. Castro, Dense, fine-grained Ba1-xSrxTiO_3 ceramics prepared by the combination of mechanosynthesized nanopowders and Spark Plasma Sintering, *Chem. Mater.* **17**, 6205 (2005).
[16] Y. Gao, V. V. Shvartsman, D. Gautam, M. Winterer and D. C. Lupascu, Nanocrystalline barium strontium titanate ceramics

synthesized via the "organosol" route and Spark Plasma Sintering, *J. Am. Ceram. Soc.* **97**, 2139 (2014).
[17]U.-C. Chung, C. Elissalde, F. Mompiou, J. Majimel, S. Gomez, C. Estournès, S. Marinel, A. Klein, F. Weill, D. Michau, S. Mornet and M. Maglione, Interface investigation in nanostructured $BaTiO_3$/silica composite ceramics, *J. Am. Ceram. Soc.* **93**, 865 (2010).
[18]U.-C. Chung, C. Elissalde, C. Estournès and M. Maglione, Controlling internal barrier in low loss $BaTiO_3$ supercapacitors, *Appl. Phys. Lett.* **94**, 072903 (2009).
[19]G. Philippot, M. Albino, R. Ephere, G. Chevallier, A. Weibel, A. Peigney, M. Deluca, C. Elissalde, M. Maglione, C. Aymonier and C. Estournès, submitted.
[20]G. Philippot, K. M. Ø. Jensen, M. Christensen, C. Elissalde, M. Maglione, B. B. Iversen and C. Aymonier, Coupling in situ synchrotron radiation with ex situ spectroscopy characterizations to study the formation of $Ba_{1-x}Sr_xTiO_3$ nanoparticles in supercritical fluids, *J. Supercrit. Fluids* **87**, 111 (2014).
[21]G. Philippot, C. Elissalde, M. Maglione and C. Aymonier, Supercritical fluid technology: A reliable process for high quality $BaTiO_3$ based nanomaterials, *Adv. Powder Technol.* **25**, 1415 (2014).
[22]S. Mornet, C. Elissalde, V. Hornebecq, O. Bidault, E. Duguet, A. Brisson and M. Maglione, Controlled growth of silica shell on $Ba_{0.6}Sr_{0.4}TiO_3$ nanoparticles used as precursors of ferroelectric composites, *Chem. Mater.* **17**, 4530 (2005).
[23]S. Mornet, C. Elissalde, O. Bidault, F. Weill, E. Sellier, O. Nguyen and M. Maglione, Ferroelectric-based nanocomposites: towards multifunctional materials, *Chem. Mater.* **19**, 987 (2007).
[24]C. Aymonier, C. Elissalde, H. Reveron, F. Weill, M. Maglione and F. Cansell, Supercritical fluid technology of nanoparticles coating for new ceramic materials, *J. Nanosci. Nanotech.* **5**, 980 (2005).
[25]R. Berthelot, B. Basly, S. Buffiere, J. Majimel, G. Chevallier, A. Weibel, A. Veillere, L. Etienne, U.-C. Chung, G. Goglio, M. Maglione, C. Estournes, S. Mornet and C. Elissalde, From core-shell $BaTiO_3$@MgO to nanostructured low dielectric loss ceramics by spark plasma sintering, *J. Mater. Chem.* **2**, 683 (2014).
[26]F. Caruso, Nanoengineering of particle surfaces, *Adv. Mater.* **13**, 11 (2001).
[27]F. Grasset, N. Labhsertwar, D. Li, D. C. Park, N. Saito, H. Haneda, O. Cador, T. Roisnel, S. Mornet, E. Duguet, J. Portier and J. Etourneau, Synthesis and magnetic characterization of zinc ferrite nanoparticles with different environments: Powder, colloidal solution and zinc ferrite silica core shell nanoparticles, *Langmuir* **18**, 8209 (2002).
[28]M. D. Sacks, N. Bozkurt and G. W. Scheiffele, Fabrication of mullite and mullite-matrix composites by transient viscous sintering of composite powders, *J. Am. Ceram. Soc.* **74**, 2428 (1991).
[29]M. T. Buscaglia, V. Buscaglia and R. Alessio, Coating of $BaCO_3$ crystals with TiO_2 versatile approach to the synthesis of $BaTiO_3$ tetragonal nanoparticles, *Chem. Mater.* **19**, 711 (2007).
[30]V. Hornebecq, C. Huber, M. Maglione, M. Antonietti and C. Elissalde, Dielectric properties of pure $(BaSr)TiO_3$ and composites with different grain sizes ranging from the nanometer to the micrometer, *Adv. Funct. Mater.* **14**, 899 (2004).
[31]D. Nuzhnyy, J. Petzelt, V. Bovtun, M. Kempa, M. Savinov, C. Elissalde, U.-C. Chung, D. Michau, C. Estournès and M. Maglione, High-frequency dielectric spectroscopy of $BaTiO_3$ Core–silica shell nanocomposites: Problem of interdiffusion, *J. Adv. Dielectr.* **1**, 309 (2011).
[32]U.-C. Chung, D. Michau, C. Elissalde, S. Li, A. Klein and M. Maglione, Evidence of diffusion at $BaTiO_3$/Silicon interfaces, *Thin Solids Films* **520**, 1997 (2012).
[33]S. Guillemet-Fritsch, Z. Valdez-Nava, C. Tenailleau, T. Lebey, B. Durand and J. Y. Chane-Ching, Colossal permittivity in ultrafine grain size $BaTiO_{3-x}$ and $Ba_{0.95}La_{0.05}TiO_{3-x}$ materials, *Adv. Mater.* **20**, 551 (2008).
[34]H. Han, C. Voisin, S. Guillemet-Fritsch, P. Dufour, C. Tenailleau, C. Turner and J. C. Nino, Origin of colossal permittivity in BaTiO3 via broadband dielectric spectroscopy, *J. Appl. Phys.* **113**, 024102 (2013).
[35]A. Artemenko, C. Elissalde, U.-C. Chung, C. Estournès, S. Mornet, I. Bykov and M. Maglione, Linking hopping conductivity to giant dielectric permittivity in oxides, *Appl. Phys. Lett.* **97**, 132901 (2010).
[36]H. Zheng, J. Wang, S. E. Lofland, S. E. Lofland, Z. Ma, L. Mohaddes-Ardabili, T. Zhao, L. Salamanca-Riba, S. R. Shinde, S. B. Ogale, F. Bai, D. Viehland, Y. Jia, D. G. Schlom, M. Wuttig, A. Roytburd and R. Ramesh, Multiferroic $BaTiO_3$-$CoFe_2O_4$ nanostructures, *Science* **303**, 661 (2004).
[37]D. Sallagoity, C. Elissalde, J. Majimel, U.-C. Chung, N. Penin, R. Berthelot, M. Maglione, V. A. Antohe, G. Hamoir, F. Abreu Araujo and L. Piraux, Synthesis and magnetic properties of Ni-$BaTiO_3$ nanocable arrays within ordered anodic alumina templates, *J. Mater. Chem. C* **3**, 107 (2015).
[38]C. Bousquet, C. Elissalde, C. Aymonier, M. Maglione, F. Cansell and J.-M. Heintz, Tuning Al_2O_3 crystallinity under supercritical fluid conditions: Effect on sintering, *J. Eur. Ceram. Soc.* **28**, 223 (2008).
[39]H. Reveron, C. Aymonier, A. Loppinet-Serani, C. Elissalde, M. Maglione and F. Cansell, Single-step synthesis of well-crystallized and pure BaTiO3 nanoparticles in supercritical fluids, *Nanotechnology* **16**, 1137 (2005).
[40]H. Reveron, C. Elissalde, C. Aymonier, O. Bidault, M. Maglione and F. Cansell, Supercritical fluid route for synthesizing crystalline barium strontium titanate nanoparticles, *J. Nanosci. Nanotechnol.* **5**, 1741 (2005).
[41]H. Reverón, C. Elissalde, C. Aymonier, C. Bousquet, M. Maglione and F. Cansell, Continuous supercritical synthesis and dielectric behavior of the whole BST solid solution, *Nanotechnology* **17**, 3527 (2006).
[42]G. Philippot, M. Albino, U.-C. Chung, M. Josse, C. Elissalde, M. Maglione and C. Aymonier, submitted.
[43]J. J. Zhang, J. W. Zhai and X. Yao, Dielectric tunable properties of low-loss $Ba_{0.4}Sr_{0.6}Ti_{1-y}Mn_yO_3$ ceramics, *Scr. Mater.* **61**, 764 (2009).
[44]L. C. Sengupta and S. Sengupta, Breakthrough advances in low loss, tunable dielectric materials, *Mater. Res. Innov.* **2**, 278 (1999).
[45]W. Chang and L. Sengupta, Ceramic ferroelectric composite material BSTO–Magnesium based for tunable microwave applications, *J. Appl. Phys.* **92**, 3941 (2002).
[46]E. A. Nenasheva, N. F. Kartenko, I. M. Gaidamaka, O. N. Trubitsyna, S. S. Redozubov, A. I. Dedyke and A. D. Kanareykin, Low loss microwave ferroelectric ceramics for high power tunable devices, *J. Eur. Ceram. Soc.* **30**, 395 (2010).
[47]S. Agrawal, R. Guo, D. Agrawal and A. S. Bhalla, Dielectric tunability of BST: MgO composites prepared by using nano particles, *Ferroelectr. Lett.* **31**, 149 (2004).

[48]G. Hu, F. Gao, L. Liu, X. Cao and Z. Liu, Microstructure and dielectric properties of $Ba_{0.6}Sr_{0.4}TiO_3$–$MgAl_2O_4$ composite ceramics, *Ceram. Int.* **37**, 1321 (2011).

[49]C. Elissalde, C. Estournes and M. Maglione, Tailoring dielectric properties of multilayer composites using spark plasma sintering, *J. Am. Ceram. Soc.* **90**, 973 (2007).

[50]U.-C. Chung, C. Elissalde, C. Estournès, M. Paté, J.-P. Ganne and M. Maglione, Low losses, highly tunable $Ba_{0.6}Sr_{0.4}TiO_3$/MgO composite, *Appl. Phys. Lett.* **92**, 042902 (2008).

[51]C. Elissalde, U.-C. Chung, A. Artemenko, C. Estournès, R. Costes, M. Paté, J. P. Ganne, S. Waechter and M. Maglione, Stoichiometry and grain boundaries control by Spark Plasma Sintering in $Ba_{0.6}Sr_{0.4}TiO_3$: Mn/MgO composites, *J. Am. Ceram. Soc.* **95**, 3239 (2012).

[52]J. Lesseur, U. C. Chung, D. Bernard, C. Estournès, M. Maglione and C. Elissalde, 3D mapping of anisotropic ferroelectric/dielectric composites, *J. Eur. Ceram. Soc.* **35**, 337 (2015).